

MoDEx: Mixture of Depth-specific Experts for Multivariate Long-term Time Series Forecasting

Hyekyung Yoon^{2*}, Minhyuk Lee^{1*}, Imseong Park³, Myungjoo Kang^{1,2,3†}

¹Department of Mathematical Sciences, Seoul National University, South Korea

²Interdisciplinary Program in Artificial Intelligence, Seoul National University, South Korea

³Research Institute of Mathematics, Seoul National University, South Korea

{yhk04150, 356min, parkis, mkang}@snu.ac.kr

Abstract

Multivariate long-term time series forecasting (LTSF) supports critical applications such as traffic-flow management, solar-power scheduling, and electricity-transformer monitoring. The existing LTSF paradigms follow a three-stage pipeline of embedding, backbone refinement, and long-horizon prediction. However, the behaviors of individual backbone layers remain underexplored. We introduce *layer sensitivity*, a gradient-based metric inspired by GradCAM and effective receptive field theory, which quantifies both positive and negative contributions of each time point to a layer’s latent features. Applying this metric to a three-layer MLP backbone reveals depth-specific specialization in modeling temporal dynamics in the input sequence. Motivated by these insights, we propose **MoDEx**, a lightweight Mixture of Depth-specific Experts, which replaces complex backbones with depth-specific MLP experts. MoDEx achieves state-of-the-art accuracy on seven real-world benchmarks—ranking first in 78% of cases—while using significantly fewer parameters and computational resources. It also integrates seamlessly into transformer variants, consistently boosting their performance and demonstrating robust generalizability as an efficient and high-performance LTSF framework.

1 Introduction

Multivariate long-term time series forecasting (LTSF) is an established field focused on modelling the joint evolution of multiple correlated variables. Accurate LTSF underpins high-impact applications such as traffic-flow management (Ji et al. 2023), solar-power scheduling (Lai et al. 2018), and electricity transformer temperature (Zhou et al. 2021). Since the introduction of the Transformer architecture (Vaswani et al. 2017) in LTSF, a variety of transformer based models have been proposed, including Informer (Zhou et al. 2021), Pyraformer (Liu et al. 2022b), Crossformer (Zhang and Yan 2023), PatchTST (Nie et al. 2023), and iTransformer (Liu et al. 2024). In parallel, CNN based methods have exploited deep convolutional filters to capture both local and hierarchical temporal patterns, yielding competitive results (Liu et al. 2022a; Wang et al. 2023; Luo and Wang 2024; Lee, Yoon, and Kang 2025). More recently, purely MLP based architectures (Zeng et al. 2023;

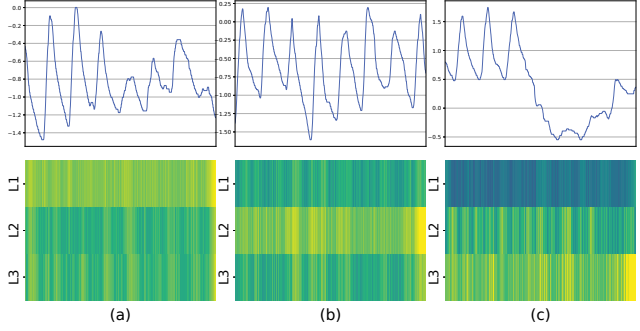


Figure 1: Let L_l be the layer sensitivity of a layer l . The top row shows the input sequence and the bottom row its sensitivity. Yellow region mark high-contribution inputs, with uniform yellow indicating global attention. The layer exhibiting global sensitivity varies with the sequence’s intrinsic periodicity and trend.

Wu et al. 2023; Han et al. 2024) have demonstrated that fully connected lightweight networks can achieve an accuracy on par with the transformer and CNN models. Despite the diversity of baseline architectures, a forecasting pipeline universally comprises three stages: (i) an embedding network that transforms raw sequences into latent representations, (ii) a deep backbone network composed of identical layers, which captures temporal dependencies and (iii) a prediction network that generates long-horizon forecasts. Since many of the aforementioned studies have focused primarily on modifying backbone layers, it is crucial to analyze the characteristics of the intermediate features produced by each backbone layer.

To analyze the properties of the backbone layers, we examine the extent to which their intermediate features are influenced by the dynamics of the input sequence. To quantify this influence, we introduce *layer sensitivity*, a gradient-based measure inspired by GradCAM (Selvaraju et al. 2017) and an analysis based on the effective receptive field (ERF) (Luo et al. 2016; Ding et al. 2022; Luo and Wang 2024). Unlike previous methods that emphasize only positive impacts, layer sensitivity computes the absolute element-wise gradient of the intermediate feature, capturing both positive and negative contributions (see details in

*These authors contributed equally.

†Corresponding author.

Section 3). Therefore, computing layer sensitivity enables us to both quantify and interpret which regions of the input sequence most significantly impact the intermediate feature of each backbone layer. Accordingly, we use layer sensitivity to investigate the behavior of each backbone layer through the following experiment. Using a three-layer MLP backbone, we build our forecasting model and compute the layer sensitivity for each layer. The heat maps in Fig. 1 reveal that layers with different depths exhibit a distinct global sensitivity to the input sequence, depending on the intrinsic periodicity and trend dynamics of the input sequence. This finding suggests that layers at different depths capture distinct dynamics within the input sequence. This, in turn, implies that layers of varying depth can serve as depth-specific experts.

Building on our findings, we argue that it is sufficient to construct the backbone layers out of Mixture-of-Experts (MoE) of lightweight MLPs varying depth. This approach eliminates the need for the heavy backbone layers typically employed in previous works. Accordingly, we introduce **MoDEx**—Mixture of Depth-specific Experts. In contrast to previous MoE-based LTSF approaches (Zeevi, Meir, and Adler 1996; Ni et al. 2024), which achieve performance gains using identical experts, MoDEx consists of simple MLP experts configured at different depths. As a result, it achieves state-of-the-art accuracy while using markedly fewer parameters and incurring significantly lower computational cost. Furthermore, substituting the self-attention module with the MoE module of MoDEx consistently improves the forecasting performance in various transformer variants, demonstrating the generalizability of the MoE module of MoDEx.

Here we summarize our key contributions as follows:

- We introduce **MoDEx**, a lightweight and computationally efficient model constructed out of simple MLPs for LTSF.
- Replacing the standard self-attention module with MoE module of MoDEx consistently improves forecasting accuracy across diverse transformer variants, highlighting its **broad generalizability**.
- We define **layer sensitivity**, a metric that quantifies the influence of the input sequence on each layer’s intermediate features. This metric captures both positive and negative contributions of the input sequence.
- **MoDEx ranks first in 78% of the evaluations across seven real-world benchmark datasets.** Moreover, on certain datasets, it achieves superior forecasting performance while using only 28% of the parameters of previous state-of-the-art models.

2 Related Works

Building on the Transformer’s success in NLP (Vaswani et al. 2017), several Transformer variants have been introduced for LTSF. Informer (Zhou et al. 2021), Pyraformer (Liu et al. 2022b), and Crossformer (Zhang and Yan 2023) optimize attention mechanisms to handle long-range and multi-scale dependencies, while iTransformer (Liu et al. 2024) refines self-attention via variable-wise routing. PatchTST (Nie et al. 2023) enhances in-

put representation through patching technique. CNN based approaches—MICN (Wang et al. 2023), SCINet (Liu et al. 2022a), and ModernTCN (Luo and Wang 2024)—improve 1-D convolutions with multi-scale decomposition or widened kernels. TimesNet (Wu et al. 2023) leverages 2D reshaping for spectral attention, and CASA (Lee, Yoon, and Kang 2025) applies CNN driven scoring for spatiotemporal context. MLP driven methods such as TSMixer (Ekambaram et al. 2023), DLinear (Zeng et al. 2023), and SOFTS (Han et al. 2024) employ lightweight linear structures. Despite these architectural differences, most methods share a three-stage pipeline—embedding, stacked backbone layers, and prediction—but rarely examine how each layer responds to input dynamics. To address this, we are motivated to propose a gradient-based sensitivity measure that reveals how depth-specific experts are differentially influenced by the input sequence.

GradCAM (Selvaraju et al. 2017) computes gradients of a target class score with respect to the final backbone feature to highlight the most influential input regions. ERF analysis (Luo et al. 2016) similarly backpropagates feature gradients to identify key input locations. RePLKNet (Ding et al. 2022) counteracts ERF locality in vision models by using large-kernel convolutions for global context, and ModernTCN (Luo and Wang 2024) applies widened CNN filters to extend ERFs and improve long-range forecasting. Inspired by these approaches, we introduce a gradient-based *layer sensitivity* metric for time series.

MoE models have been actively explored for LTSF. The early work (Zeevi, Meir, and Adler 1996) laid the theoretical foundation for applying MoE to autoregressive models. MoLE (Ni et al. 2024) replaces the backbone layer with lightweight and linear-centric experts blended by a router. Although these approaches improve accuracy, they employ uniform expert architectures. In contrast, MoDEx utilizes varied depth-specific MLP experts, assigning specialized roles to each layer to promote diverse intermediate representations and achieve better accuracy and efficiency with fewer parameters and lower computation.

3 Method

3.1. Notations

Let L , H , and D be the input sequence length, the ground truth label, and the hidden dimension, respectively. Many prior methods first embed the input sequence $x \in \mathbb{R}^L$ and then propagate the resulting feature through a backbone network of M identical layers. The resultant latent feature is subsequently processed by a prediction network to predict the output sequence $y \in \mathbb{R}^H$. We denote the embedding network by $f_e : \mathbb{R}^L \rightarrow \mathbb{R}^D$, each backbone layer by $f_i : \mathbb{R}^D \rightarrow \mathbb{R}^D$ for $i = 1, \dots, M$, and the prediction network by $f_p : \mathbb{R}^D \rightarrow \mathbb{R}^H$. For brevity, define

$$g_0 := f_e, \quad g_i := f_i, \quad g_{M+1} := f_p, \quad (1)$$

$$G_l := g_l \circ g_{l-1} \circ \dots \circ g_0. \quad (2)$$

3.2. Input-Dependent Backbone Layer Sensitivity to Sequence Periodicity and Trend Dynamics

We propose a novel approach, drawing on GradCAM (Selvaraju et al. 2017), ERF (Luo et al. 2016), RepLKNNet (Ding et al. 2022), and ModernTCN (Luo and Wang 2024), to investigate the impact of input dynamics on backbone layers. At first, to examine the sensitivity of backbone layers to input perturbations, we compute the gradient of l -th layer’s output feature with respect to the j -th input coordinate as follows:

$$\frac{\partial G_l}{\partial x_j} = \left(\prod_{i=1}^l \frac{\partial g_i}{\partial g_{i-1}} \right) \frac{\partial g_0}{\partial x_j} = \left(\prod_{i=1}^l \frac{\partial g_i}{\partial g_{i-1}} \right) \frac{\partial g_0}{\partial x} e_j, \quad (3)$$

where $\frac{\partial g_i}{\partial g_{i-1}} \in \mathbb{R}^{D \times D}$ for $i = 1, \dots, l$ ($l \leq M$) and $\frac{\partial g_0}{\partial x} \in \mathbb{R}^{D \times L}$ are the Jacobian matrices of the layer mappings, and $e_j \in \mathbb{R}^L$ is the j -th standard basis vector. Next, the sensitivity matrix of the l -th layer to input perturbations is represented by a $D \times L$ matrix defined as the product of the following Jacobian matrices:

$$\frac{\partial G_l}{\partial x} = \left(\prod_{i=1}^l \frac{\partial g_i}{\partial g_{i-1}} \right) \frac{\partial g_0}{\partial x} \in \mathbb{R}^{D \times L}. \quad (4)$$

To determine how each input component contributes to the l -th layer’s output features in equation (4), we compute the row-wise mean of the sensitivity matrix. To capture both positive and negative contributions, we take the absolute value before averaging. Now, we define **the l -th layer sensitivity** $S_l(x) \in \mathbb{R}^L$ with respect to x as

$$S_l(x) = \frac{1}{D} \sum_{i=1}^D \left| \text{row}_i \left(\frac{\partial G_l}{\partial x} \right) \right|_{\text{abs}}, \quad (5)$$

where $\text{row}_i(*)$ denotes the i -th row of $*$ and $|\cdot|_{\text{abs}}$ is the element-wise absolute value function.

In two respects, our derivation of S_l departs from established input-attribution techniques—namely GradCAM and ERF based methods. First, these approaches differ in both their backpropagation targets and the way they extract scores from the sensitivity matrix. GradCAM computes contributions by backpropagating from the final network output for a given classification label. ERF based methods limit their analysis to the central spatial position of the final backbone feature map—that is, the $[D/2]$ -th row of the sensitivity matrix. By contrast, we analyze intermediate feature maps and aggregate input influence via a row-wise mean over all D rows. Second, prior works consider only positive contributions by discarding negative entries in the sensitivity matrix. We instead capture both positive and negative effects by taking the element-wise absolute value before averaging.

To perform our sensitivity analysis, we investigate how each layer responds to variations in the input sequence (Fig. 1). We construct the embedding network, each backbone layer, and the prediction network using GELU activations and linear mappings. The backbone network comprises three such backbone layers. After constructing the

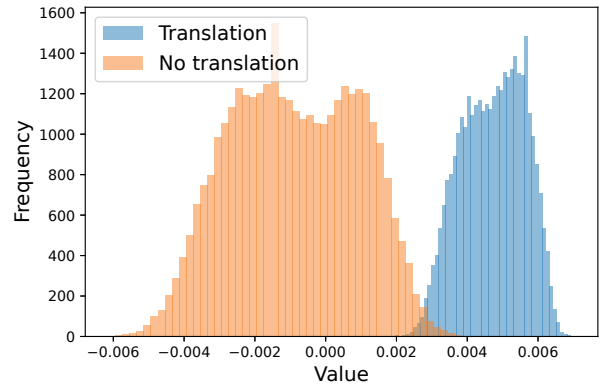


Figure 2: Distribution of coordinate-wise mean feature values on the ETTm2 dataset. Applying the Learnable Translation (Blue) shifts these mean values overall toward the positive direction compared to the no-translation baseline (Orange).

forecasting pipeline, we observe that the intermediate features of each layer exhibit partially overlapping receptive regions with respect to the input sequence. However, depending on the intrinsic periodicity and trend dynamics of the input sequence, different layers exhibit the distinct highest sensitivity across the entire input sequence. This observation indicates that each depth-specific MLP acts as an **expert** for particular input patterns. Based on it, we propose a new framework which is depth-specific MLP MoE, detailed in Section 3.4.

3.3. Learnable Translation of Input Features

Before presenting our main architecture, we introduce a technique to improve model performance. ReLU-like activations zero out negative values and thus may discard informative intermediate features. This issue is further exacerbated by the generally used normalization technique (Kim et al. 2022) in LTSF, which normalizes both input and output distributions to a standard normal. To address this bias, we incorporate a learnable translation in the MLP architecture. While minimizing the loss during training, we track whether each input feature element is adjusted in a positive or negative direction. Consequently, this shifts the feature distribution positively so that most values become non-negative on average (Fig. 2). Furthermore, incorporating a learnable translation enhances predictive performance (Experimental details in Appendix A.2). These findings empirically validate the efficacy of the learnable translation. Accordingly, **our model integrates this learnable translation to realign input features and mitigate the bias introduced by conventional normalization.**

3.4. MoDEx: Mixture of Depth-specific Experts for Multivariate Long-term Time Series Forecasting

To construct an efficient and lightweight MLP based model, we propose the backbone layer as a **Mixture of Depth-specific Experts (MoDEx)**. This architecture exploits the

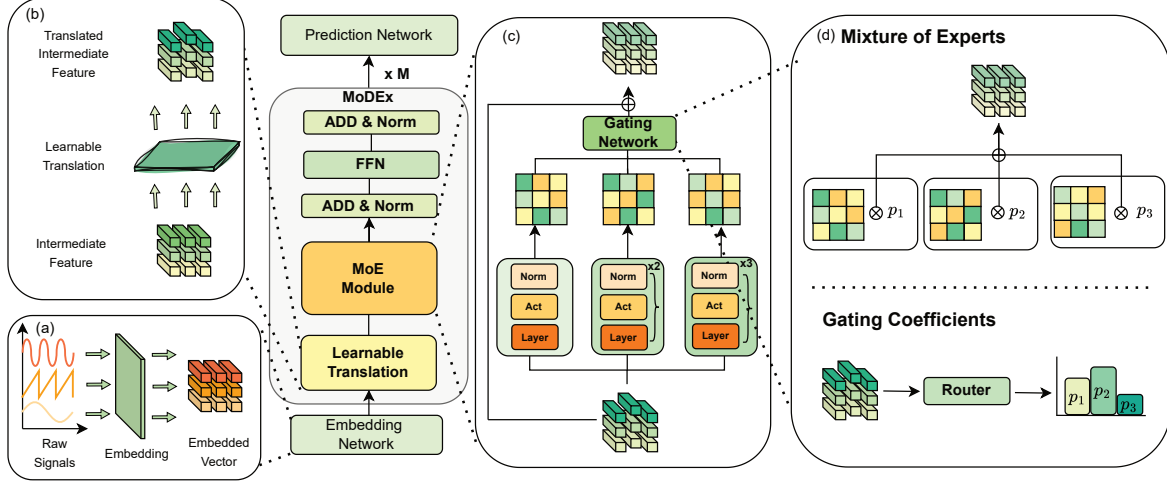


Figure 3: Main architecture of MoDEx. (a) The input sequence is linearly embedded. (b) The embedded vectors pass through a learnable transition layer. (c) MoDEx module comprises three depth-specific MLP experts. (d) Expert outputs are weighted by gating coefficients and aggregated to produce the final prediction.

	MoDEx	SOFTS	iTransformer	PatchTST	Transformer
Complexity	$O(NL + NH)$	$O(NL + NH)$	$O(N^2 + NL + NH)$	$O(NL^2 + NH)$	$O(NL + L^2 + HL + NH)$
Parameters	3329K	3574K	4833K	6903K	10518K
FLOPs	895.2M	933.9M	3139.70M	49005.88M	2372.12M

Table 1: Complexity comparison on Solar datasets among vanilla Transformer, PatchTST, iTransformer, and SOFTS as functions of window length L , the number of variates N , and horizon H .

specialized sensitivity of each expert to distinct input patterns. Based on the layer sensitivity, we observe that MLPs of different depths exhibit distinct sensitivities to the input sequence’s intrinsic periodicity and trend dynamics. Accordingly, we configure depth-specific MLPs to serve as experts within MoDEx framework. Because empirical results show that three experts is sufficient, we limit each module to three experts to maintain a lightweight design (see Appendix A.4 for details).

We now present an explanation of the operation of MoE module of MoDEx. We denote the input feature of a backbone layer by z and the corresponding depth-specific experts by h_j ($j = 1, 2, 3$) and compute a gating coefficient p_j over the each expert via a router. The gated experts’ outputs are then aggregated and added residually to the original feature. We denote the final output of the MoE architecture by \tilde{z} , given by the following equation:

$$\tilde{z} = z + \sum_{j=1}^3 p_j(z) h_j(z). \quad (6)$$

With this MoE module, the detailed construction is described in Fig. 3. Finally the forecasting pipeline for the input sequence is described by the following equations:

$$y = G_{M+1}(x) = (g_{M+1} \circ g_M \circ \dots \circ g_0)(x). \quad (7)$$

In addition, MoE module of MoDEx can be seamlessly integrated into Transformer architectures, demonstrating its generalizability. As defined earlier equation (6), MoE module of MoDEx can operate independently and serve as a drop-in replacement for a Transformer’s self-attention block. Accordingly, we construct each backbone layer f_i by replacing its self-attention mechanism with MoE module (Fig. 3). A detailed discussion is provided in Section 4.3.

Complexity Analysis MoDEx is an efficient algorithm that exhibits linear complexity. Table 1 summarizes the detailed computational complexity of each baseline and reports the model parameter counts and FLOPs on a Solar dataset. Although our method has the same asymptotic complexity of SOFTS, it uses smaller hidden dimension and fewer layers. As a result, it requires substantially fewer parameters and lower computational cost, as shown in Table 1. For a detailed analysis of the practical effects of its linear complexity on memory usage, inference time, parameter counts, and FLOPs, see Sections 4.2 and 4.4. The computational complexity is computed as follows: RevIN requires $O(NL)$, series embedding $O(NLD)$, and the MLP $O(ND^2)$. Consequently, the overall complexity is $O(NL + NLD + ND^2 + NDH)$ which scales linearly in N , L , and H . Since D is treated as a constant and $L, H \gg 1$ in LTSF, the dominant cost reduces to $O(N(L + H))$.

Methods Metric	MoDEx		SOFTS		iTTransformer		PatchTST		TSMixer		Crossformer		TimesNet		DLinear	
	MSE	MAE	MSE	MAE	MSE	MAE	MSE	MAE	MSE	MAE	MSE	MAE	MSE	MAE	MSE	MAE
ETTh1	0.439	0.436	0.449	0.442	0.454	0.447	0.453	0.446	0.463	0.452	0.529	0.522	0.458	0.450	0.456	0.452
ETTh2	0.379	0.404	0.373	0.400	0.383	0.407	0.385	0.410	0.401	0.417	0.942	0.684	0.414	0.427	0.559	0.515
ETTm1	0.392	0.401	0.393	0.403	0.407	0.410	0.396	0.406	0.398	0.407	0.513	0.496	0.400	0.406	0.474	0.453
ETTm2	0.285	0.325	0.287	0.330	0.288	0.332	0.287	0.330	0.289	0.333	0.757	0.610	0.291	0.333	0.350	0.401
ECL	0.172	0.263	0.174	0.264	0.178	0.270	0.189	0.276	0.186	0.287	0.244	0.334	0.192	0.295	0.212	0.300
Weather	0.256	0.277	0.255	0.278	0.258	0.278	0.256	0.279	0.256	0.279	0.259	0.315	0.259	0.287	0.265	0.317
Solar	0.228	0.253	0.229	0.256	0.233	0.262	0.236	0.266	0.236	0.297	0.641	0.639	0.301	0.319	0.330	0.401
1st count	11		3		0		0		0		0		0		0	

Table 2: Forecasting performance for multivariate time series with a fixed lookback window $L = 96$ and prediction horizons $H \in \{96, 192, 336, 720\}$. Bold values are the best performance, while underlined values indicate the second-best.

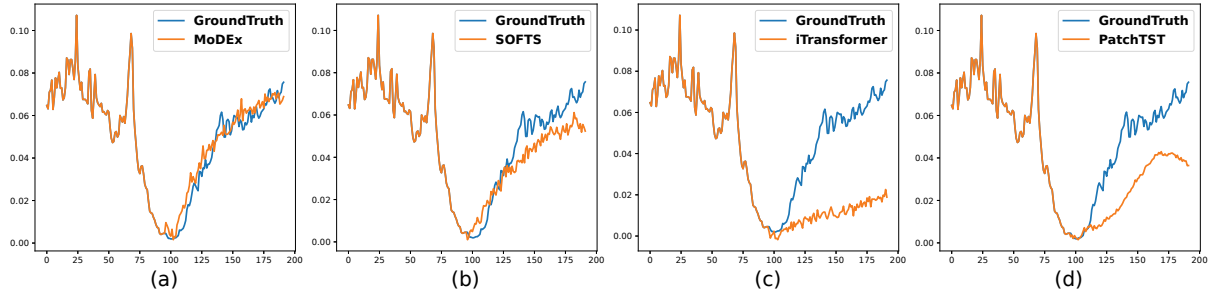


Figure 4: Comparison of forecasting performance on the Weather dataset: (a) MoDEx (Ours), (b) SOFTS, (c) iTTransformer, and (d) PatchTST.

4 Experiments

4.1. Setup

Datasets We evaluate our method on seven standard LTSF benchmarks (Zhou et al. 2021): the ETT series (ETTh1, ETTh2, ETTm1, ETTm2), Weather, Solar, and Electricity. Full dataset statistics and descriptions are provided in Appendix A.1.

Baselines We compare against seven recent transformer and MLP based models: SOFTS (Han et al. 2024), iTTransformer (iTrans) (Liu et al. 2024), PatchTST (TST) (Nie et al. 2023), TSMixer (Wang et al. 2024), Crossformer (Cross) (Zhang and Yan 2023), TimesNet (Wu et al. 2023), and DLinear (Zeng et al. 2023).

Experimental Setup For estimating point wise accuracy, performance is measured using Mean Squared Error (MSE) and Mean Absolute Error (MAE). All experiments use an input window of length $L = 96$ and prediction lengths $H \in \{96, 192, 336, 720\}$.

4.2. Multivariate Forecasting Results

Table 2 summarizes the average performance across four prediction lengths, showing MoDEx achieves the lowest MSE and MAE on seven benchmark datasets and leading in 11 cases. Fig. 4 highlights MoDEx’s superior forecasting accuracy on the Weather dataset with predictions closely aligned to ground truth, outperforming iTTransformer,

Model	MSE(\downarrow)	MAE(\downarrow)	Param.(\downarrow)	FLOPs(\downarrow)	infer.(s)(\downarrow)
SOFTS	0.449	0.442	824K	16.71M	0.479
iTrans	0.454	0.447	255K	5.60M	0.609
PatchTST	0.453	0.446	5226K	559.88M	0.586
TSMixer	0.463	0.452	119K	33.07M	1.007
Cross	0.529	0.522	42339K	10509.49M	2.584
MoDEx	0.439	0.436	280K	3.83M	0.446

Table 3: Performance on the ETTh1 dataset, averaged across all horizons. MoDEx achieves the lowest errors, lowest FLOPs, and fastest inference time, while using the second fewest parameters.

SOFTS, and PatchTST—SOFTS captures trends but deviates more, and iTTransformer and PatchTST diverge noticeably. Table 3 further demonstrates MoDEx’s performance on ETTh1, surpassing baselines with an average MSE of 0.439 and MAE of 0.436. Despite this, MoDEx remains highly efficient, using the second fewest parameters (280K), the lowest computational cost (3.83 MFLOPs), and the fastest inference time (0.446 sec/sample), underscoring its strength as a lightweight and accurate forecasting model.

4.3. Generalizability of MoE module of MoDEx

To evaluate the generalizability of MoE module as a replacement for self-attention module, we substitute it in

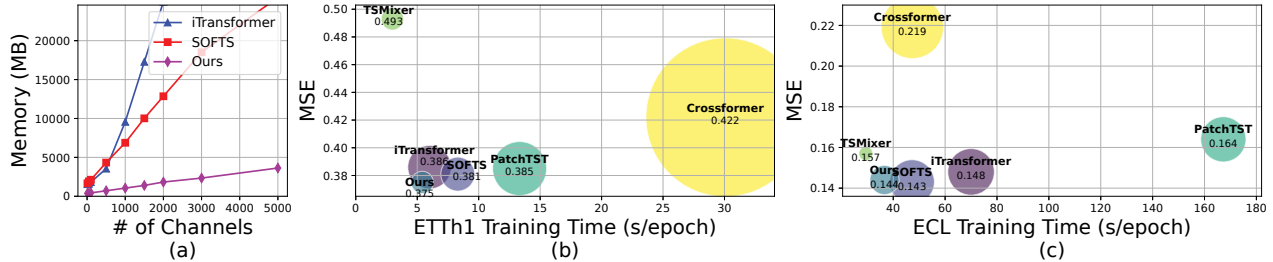


Figure 5: (a) Memory consumption versus the number of variates, showing MoDEX’s linear scalability and lower memory usage than SOFTS and iTransformer. (b) and (c) bubble plots on the ETTh1 (batch size: 32) and Electricity (batch size: 16) datasets with input/prediction length of 96; bubble size indicates model size. MoDEX achieves a strong trade-off between speed and accuracy on ETTh1, and maintains the second smallest parameter count on Electricity despite a marginal MSE gap.

Model	Comp.	ETTh1		ETTh2		ETTm1		ETTm2	
		MSE	MAE	MSE	MAE	MSE	MAE	MSE	MAE
Trans	Attn	0.482	0.465	0.522	0.481	0.407	0.417	0.369	0.398
	Ours	0.474	0.459	0.493	0.469	0.407	0.421	0.352	0.389
iTrans	Attn	0.454	0.447	0.383	0.407	0.407	0.410	0.288	0.332
	Ours	0.443	0.436	0.380	0.405	0.394	0.401	0.258	0.329
TST	Attn	0.453	0.446	0.385	0.410	0.396	0.406	0.287	0.330
	Ours	0.447	0.441	0.381	0.402	0.388	0.402	0.286	0.331

Table 4: Performance of MoDEX as a plug-in replacement for self-attention in Transformer variants. Replacing self-attention with MoDEX consistently improves forecasting accuracy across four benchmark datasets.

Data	Pred.	96		192		336		720	
		MSE	MAE	MSE	MAE	MSE	MAE	MSE	MAE
ETTh1	MoLE _D	0.398	0.413	0.462	0.448	0.514	0.479	0.521	0.504
	MoLE _R	0.393	0.400	0.440	0.428	0.504	0.468	0.543	0.502
	Ours	0.375	0.397	0.428	0.426	0.479	0.452	0.475	0.471
ETTm1	MoLE _D	0.355	0.387	0.427	0.432	0.469	0.461	0.528	0.492
	MoLE _R	0.363	0.382	0.391	0.409	0.417	0.418	0.500	0.474
	Ours	0.328	0.365	0.370	0.385	0.405	0.407	0.468	0.447

Table 5: Performance Comparison with MoLE across prediction length (Pred.). MoDEX consistently outperforms MoLE, which relies solely on identical experts.

several Transformer based models with MoE module of MoDEX. Models used for experiments are the vanilla Transformer (Vaswani et al. 2017), iTransformer (Liu et al. 2024), and PatchTST (Nie et al. 2023). As shown in Table 4, incorporating MoDEX leads to improved performance across four different benchmark datasets compared to the original models. Notably, despite the differing tokenization strategies employed by these models—such as point-wise embedding, patch embedding, and variate-independent embedding (detailed in Appendix B)—MoDEX can be integrated seamlessly with all of them. This demonstrates not only its flexibility across diverse tokenization schemes but also its ability to enhance the forecasting performance of various Transformer architectures.

4.4. Model Efficiency Analysis

To demonstrate the computational efficiency of MoDEX, we compare our method with several baseline models, specifically iTransformer and SOFTS. As shown in Fig. 5(a), MoDEX shows linear memory usage as the number of input channels increases, indicating stable scalability and efficient use of computational resources. In contrast, iTransformer requires quadratic memory growth, which limits its practicality for high-dimensional inputs. While SOFTS demonstrates a similar linear trend, it shows a noticeable surge in memory consumption as the input channel increases. In Fig. 5(b), although TSMixer has the smallest model size, it shows relatively high MSE. By contrast, MoDEX achieves the lowest MSE while maintaining a compact architecture. In Fig. 5(c), SOFTS achieves the lowest MSE, and TSMixer retains the smallest model size; however, MoDEX demonstrates a well-balanced trade-off between model complexity and the best on ETTh1 and second best on Electricity dataset. These findings highlight the computational efficiency and practical effectiveness of MoDEX in LTSF.

4.5. Comparison with Mixture-of-Experts Baselines

Among LTSF baselines, MoLE (Ni et al. 2024) is a directly comparable MoE model. MoLE employs homogeneous and linear-centric experts and derives gating coefficients from time stamps. Specifically, we denote the DLInear (Zeng et al. 2023) based variant as MoLE_D and the RMLP (Li et al. 2023) based variant as MoLE_R. We compare MoDEX against MoLE_D and MoLE_R on the ETTh1 and ETTm1 datasets across multiple forecasting horizons in Table 5. In every case, MoDEX consistently achieves superior accuracy. Since both frameworks use simple MLP based experts, these results indicate that depth-specific expert mixture provides enhanced forecasting performance.

4.6. Feature Diversity in MoDEX

In this section, we empirically show that MoDEX yields greater feature diversity than a MoE model employing exclusively identical 3-layer MLP experts (hereafter referred to as the homogeneous MoE model). On the ETTm2 dataset, we compare the intermediate feature distributions produced by MoDEX to those of this homogeneous MoE model. For

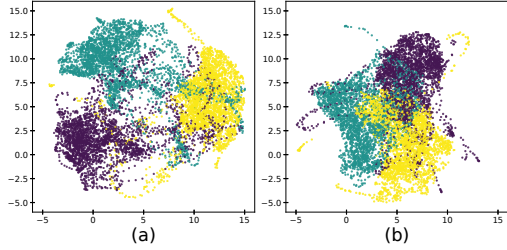


Figure 6: (a) Separate intermediate features captured by individual expert in MoDEx, highlighting its ability to specialize representations within each expert. (b) Clustered intermediate features from the homogeneous MoE model.

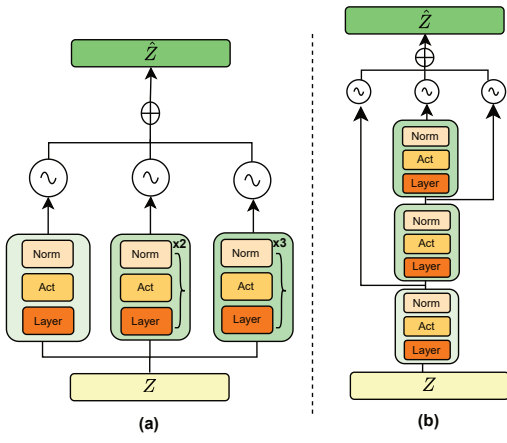


Figure 7: (a) MoDEx: a parallel MoE with three depth-specific MLP experts. (b) Dense: a sequential MoE applied across layers of a single three-layer MLP.

each input sequence, the output features of the experts are projected in two dimensions via UMAP (McInnes, Healy, and Melville 2018). As shown in Fig. 6(a), the experts of MoDEx generate distinctly varied feature distributions for identical inputs. In contrast, the homogeneous MoE model produces more tightly clustered outputs (Fig. 6(b)). The UMAP projection reveals that MoDEx’s depth-specific experts occupy multiple and well-separated clusters in feature space, each corresponding to different temporal characteristics of the input.

4.7. Efficient Architectural Alternatives

MoDEx employs three experts in a MoE framework, where each expert comprises an MLP of identical structure but differing depth. By sharing weights across these depth-specific experts, we can preserve their specialized sensitivities while reducing model parameters and computational cost. Although this architecture differs from DenseNet (Huang et al. 2017), we refer to this variant as *Dense* for convenience, since it similarly exploits intermediate feature reuse. As shown in Fig. 7, MoDEx uses a parallel MoE, whereas Dense applies MoE sequentially on a single three-layer MLP. For performance comparison, we evaluate both Dense

Data	Comp.	MSE	MAE	Param.	FLOPs	infer.(s)
ETTh1	MoDEx	0.439	0.436	280K	3.83M	0.446
	Dense	0.445	0.441	230K	3.12M	0.442
	Impr.	+1.36%	+1.14%	-17.85%	-18.54%	-0.89%
ETTh2	MoDEx	0.379	0.404	940K	12.80M	0.765
	Dense	0.382	0.406	808K	10.92M	0.684
	Impr.	+0.79%	+0.49%	-14.04%	-14.69%	-13.96%
ETTm1	MoDEx	0.392	0.401	644K	8.74M	3.379
	Dense	0.400	0.406	528K	7.10M	3.372
	Impr.	+2.30%	+1.24%	-18.01%	-18.76%	-0.21%
ETTm2	MoDEx	0.285	0.325	214K	2.91M	1.549
	Dense	0.285	0.329	164K	2.20M	1.454
	Impr.	+0.00%	+1.23%	-23.36%	-24.39%	-6.13%

Table 6: MoDEx vs. Dense variant: Despite higher complexity, MoDEx improves accuracy by up to 2.3% on ETTm1 and remains competitive across four benchmarks.

and MoDEx on the ETT series and report the average accuracy across forecasting horizons. For efficiency assessment, we measure the number of parameters, FLOPs, and inference time (Table 6). While Dense incurs a slight performance degradation, it achieves substantial reductions in model size and computation: parameters decrease by up to 23.36%, FLOPs by 24.39%, and inference time by 13.96%. In contrast, the worst-case increases in MSE and MAE are only 2.3% and 1.24%, respectively. These findings indicate that the Dense-like architecture may be preferred over MoDEx, when efficiency is paramount.

5 Conclusion

In this study, we explore behaviors of each expert in backbone layer by examining how intermediate features respond to input-sequence dynamics. We introduce layer sensitivity, a gradient-based metric that aggregates element-wise absolute gradients to capture both positive and negative influences. Our analysis reveals that layers at different depths exhibit varying sensitivity to the input sequence’s intrinsic periodicity and trend dynamics, inspiring the construction of MoDEx—Mixture of Depth-specific Experts—composed of lightweight MLPs. MoDEx outperforms existing methods, ranking first on 78% of 14 results across seven benchmarks, all while requiring significantly fewer parameters and lower computational cost. Furthermore, it serves as a drop-in replacement for self-attention in Transformer variants, consistently boosting accuracy while maintaining its generalizability and efficiency.

References

Ding, X.; Zhang, X.; Han, J.; and Ding, G. 2022. Scaling up your kernels to 31x31: Revisiting large kernel design in cnns. In *Proceedings of the IEEE/CVF conference on computer vision and pattern recognition*, 11963–11975.

Ekambaram, V.; Jati, A.; Nguyen, N.; Sinthong, P.; and Kalagnanam, J. 2023. Tsmixer: Lightweight mlp-mixer model for multivariate time series forecasting. In *Proceed-*

ings of the 29th ACM SIGKDD conference on knowledge discovery and data mining, 459–469.

Han, L.; Chen, X.-Y.; Ye, H.-J.; and Zhan, D.-C. 2024. SOFTS: Efficient Multivariate Time Series Forecasting with Series-Core Fusion. In Globerson, A.; Mackey, L.; Belgrave, D.; Fan, A.; Paquet, U.; Tomczak, J.; and Zhang, C., eds., *Advances in Neural Information Processing Systems*, volume 37, 64145–64175. Curran Associates, Inc.

Huang, G.; Liu, Z.; Van Der Maaten, L.; and Weinberger, K. Q. 2017. Densely connected convolutional networks. In *Proceedings of the IEEE conference on computer vision and pattern recognition*, 4700–4708.

Ji, J.; Wang, J.; Huang, C.; Wu, J.; Xu, B.; Wu, Z.; Zhang, J.; and Zheng, Y. 2023. Spatio-temporal self-supervised learning for traffic flow prediction. In *Proceedings of the AAAI conference on artificial intelligence*, volume 37, 4356–4364.

Kim, T.; Kim, J.; Tae, Y.; Park, C.; Choi, J.-H.; and Choo, J. 2022. Reversible Instance Normalization for Accurate Time-Series Forecasting against Distribution Shift. In *International Conference on Learning Representations*.

Lai, G.; Chang, W.-C.; Yang, Y.; and Liu, H. 2018. Modeling long-and short-term temporal patterns with deep neural networks. In *The 41st international ACM SIGIR conference on research & development in information retrieval*, 95–104.

Lee, M.; Yoon, H.; and Kang, M. 2025. CASA: CNN Autoencoder-based Score Attention for Efficient Multivariate Long-term Time-series Forecasting. *arXiv preprint arXiv:2505.02011*.

Li, Z.; Qi, S.; Li, Y.; and Xu, Z. 2023. Revisiting long-term time series forecasting: An investigation on linear mapping. *arXiv preprint arXiv:2305.10721*.

Liu, M.; Zeng, A.; Chen, M.; Xu, Z.; LAI, Q.; Ma, L.; and Xu, Q. 2022a. SCINet: Time Series Modeling and Forecasting with Sample Convolution and Interaction. In Oh, A. H.; Agarwal, A.; Belgrave, D.; and Cho, K., eds., *Advances in Neural Information Processing Systems*.

Liu, S.; Yu, H.; Liao, C.; Li, J.; Lin, W.; Liu, A. X.; and Dustdar, S. 2022b. Pyraformer: Low-Complexity Pyramidal Attention for Long-Range Time Series Modeling and Forecasting. In *International Conference on Learning Representations*.

Liu, Y.; Hu, T.; Zhang, H.; Wu, H.; Wang, S.; Ma, L.; and Long, M. 2024. iTransformer: Inverted Transformers are Effective for Time Series Forecasting. *International Conference on Learning Representations (ICLR)*. Accepted as a conference paper at ICLR 2024.

Luo, D.; and Wang, X. 2024. ModernTCN: A Modern Pure Convolution Structure for General Time Series Analysis. In *Proceedings of the Twelfth International Conference on Learning Representations (ICLR)*. Published at ICLR 2024.

Luo, W.; Li, Y.; Urtasun, R.; and Zemel, R. 2016. Understanding the effective receptive field in deep convolutional neural networks. *Advances in neural information processing systems*, 29.

McInnes, L.; Healy, J.; and Melville, J. 2018. UMAP: Uniform Manifold Approximation and Projection for Dimension Reduction. *stat*, 1050: 6.

Ni, R.; Lin, Z.; Wang, S.; and Fanti, G. 2024. Mixture-of-linear-experts for long-term time series forecasting. In *International Conference on Artificial Intelligence and Statistics*, 4672–4680. PMLR.

Nie, Y.; Nguyen, N. H.; Sinthong, P.; and Kalagnanam, J. 2023. A Time Series is Worth 64 Words: Long-term Forecasting with Transformers. In *The Eleventh International Conference on Learning Representations*.

Selvaraju, R. R.; Cogswell, M.; Das, A.; Vedantam, R.; Parikh, D.; and Batra, D. 2017. Grad-cam: Visual explanations from deep networks via gradient-based localization. In *Proceedings of the IEEE international conference on computer vision*, 618–626.

Vaswani, A.; Shazeer, N.; Parmar, N.; Uszkoreit, J.; Jones, L.; Gomez, A. N.; Kaiser, Ł.; and Polosukhin, I. 2017. Attention is all you need. *Advances in neural information processing systems*, 30.

Wang, H.; Peng, J.; Huang, F.; Wang, J.; Chen, J.; and Xiao, Y. 2023. MICN: Multi-scale Local and Global Context Modeling for Long-term Series Forecasting. In *The Eleventh International Conference on Learning Representations*.

Wang, S.; Wu, H.; Shi, X.; Hu, T.; Luo, H.; Ma, L.; Zhang, J. Y.; and Zhou, J. 2024. Timemixer: Decomposable multi-scale mixing for time series forecasting. Published at ICLR 2024.

Wu, H.; Hu, T.; Liu, Y.; Zhou, H.; Wang, J.; and Long, M. 2023. TimesNet: Temporal 2D-Variation Modeling for General Time Series Analysis. In *The Eleventh International Conference on Learning Representations*.

Zeevi, A.; Meir, R.; and Adler, R. 1996. Time series prediction using mixtures of experts. *Advances in neural information processing systems*, 9.

Zeng, A.; Chen, M.; Zhang, L.; and Xu, Q. 2023. Are transformers effective for time series forecasting? In *Proceedings of the AAAI conference on artificial intelligence*, volume 37, 11121–11128.

Zhang, Y.; and Yan, J. 2023. Crossformer: Transformer Utilizing Cross-Dimension Dependency for Multivariate Time Series Forecasting. In *The Eleventh International Conference on Learning Representations*.

Zhou, H.; Zhang, S.; Peng, J.; Zhang, S.; Li, J.; Xiong, H.; and Zhang, W. 2021. Informer: Beyond efficient transformer for long sequence time-series forecasting. In *Proceedings of the AAAI conference on artificial intelligence*, volume 35, 11106–11115.